Rare charm decays at LHCb

Chris Thomas (Oxford University)

On behalf of the LHCb collaboration

Beauty 2013, Bologna

10 April 2013

The LHCb detector

Single arm forward spectrometer covering $2 < \eta < 5$.

Designed to study heavy flavour physics.

Large charm cross section:

$\sigma(c\bar{c}) = 1419 \pm 12(\text{stat.}) \pm 116(\text{syst.}) \pm 65(\text{frag.})\ \mu\text{b}^*$ [LHCb-PAPER-2012-041].

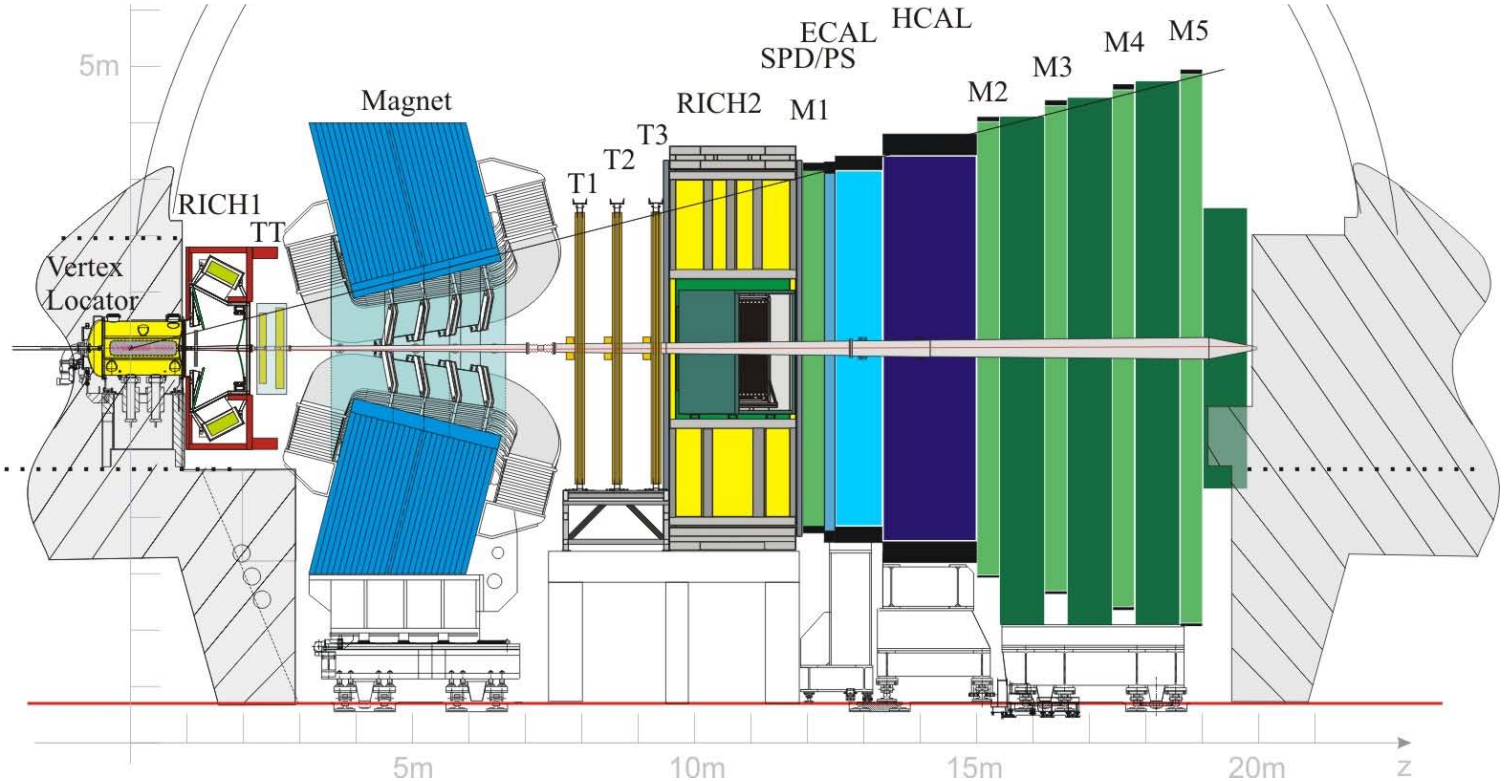

*Determined for the kinematic range $\mathbf{p}_\text{T} < 8$ GeV/c, $2.0 < y < 4.5$.

The LHCb detector

Excellent vertex detection, tracking and PID.

Flexible trigger, highly efficient on *c* and *b* decays.

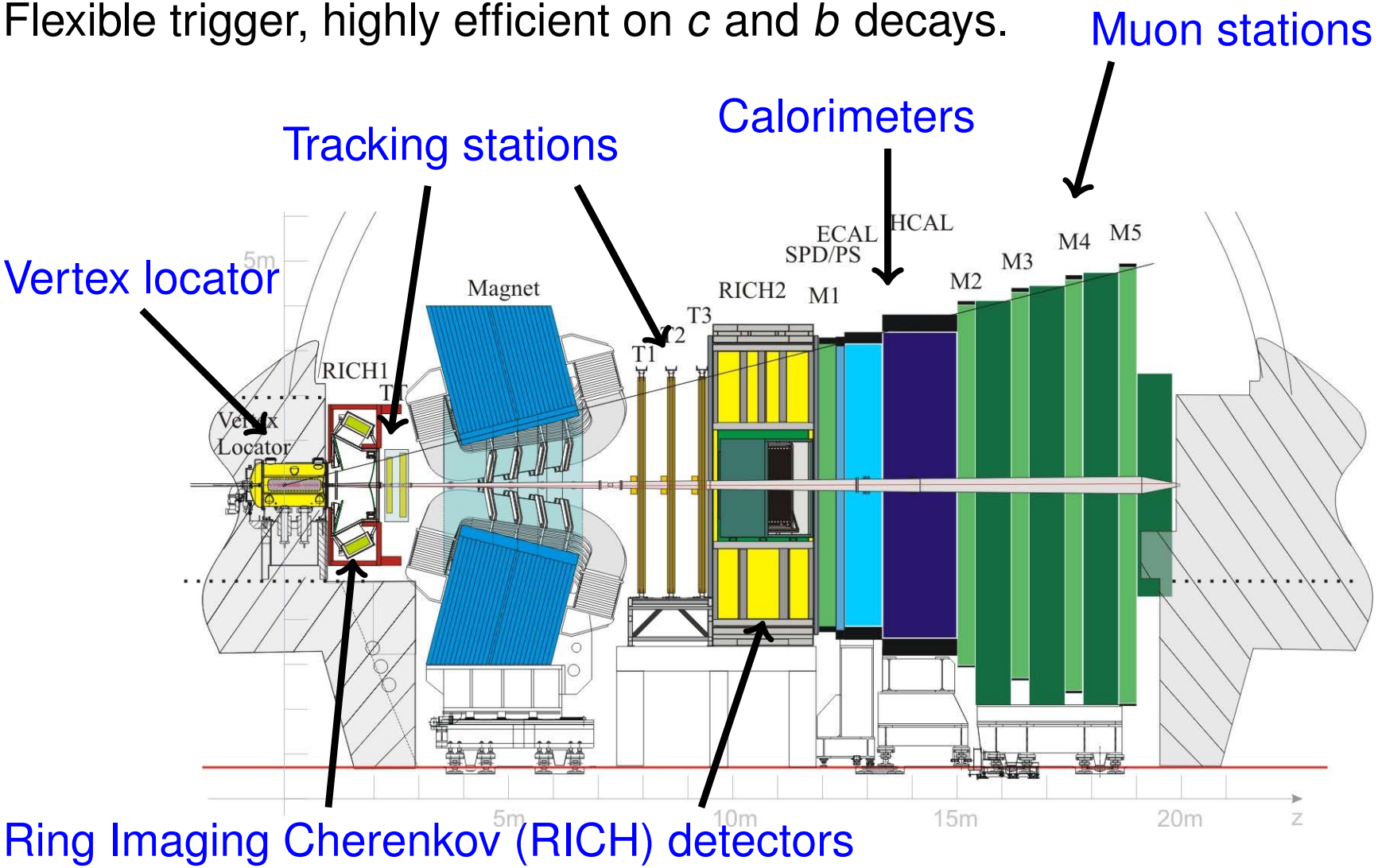

LHCb data taking

Very successful data taking throughout run.

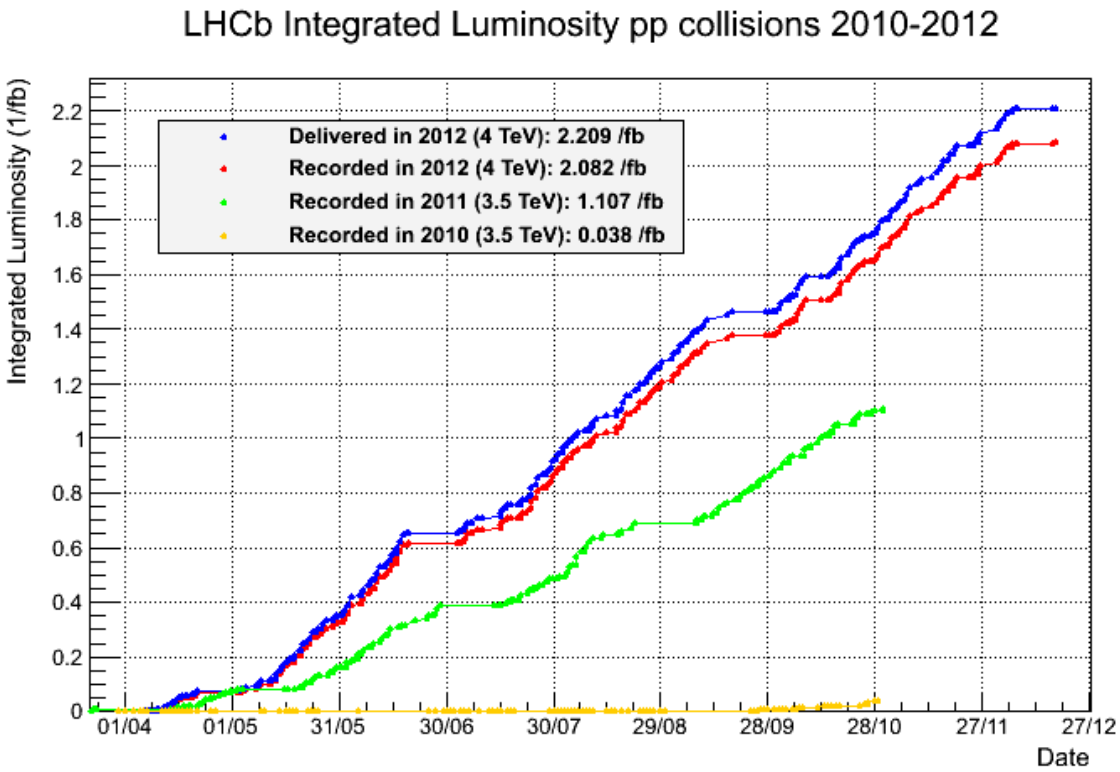

2012: 2 fb^{-1}

2011: 1 fb^{-1}

Data taking efficiency $> 93\%$.

Typical instantaneous luminosity 2–4 $\times 10^{32}$ cm^{-2} s^{-1}, exceeding design.

Luminosity levelling used to keep inst. lumi. ~constant over fill.

Rare charm decays at LHCb

'Rare' indicates decays that occur only at loop level.
Flavour-changing neutral currents (FCNCs) highly suppressed in the SM.
GIM suppression particularly significant in D decays.
Opportunity to probe u-type quark couplings in EW penguins.

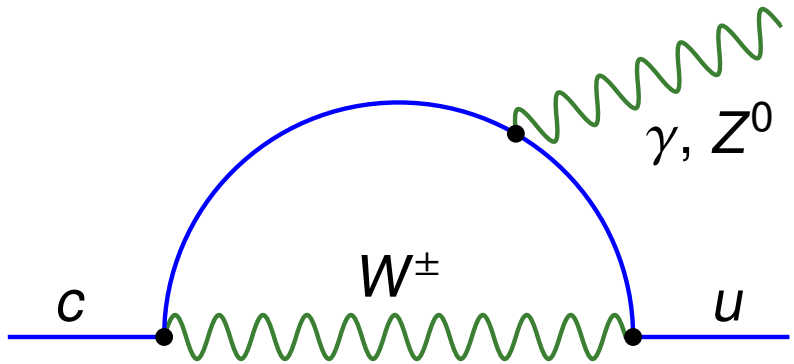

Some BSM contributions can enhance branching fractions, e.g. $\not{R}_P$ SUSY
[PRD 66: 014009 (2002)], [Ann. Rev. Nucl. Part. Sci. 53: 431 (2003)].
Precision measurements of rare decays could therefore reveal the presence of any BSM physics.
For rare B decays at LHCb, see talk by F. Dettori.

Rare charm decays at LHCb

Will discuss two searches for rare charm decays at LHCb:

1. $D^0 \to \mu^+\mu^-$,
2. $D^{\pm}_{(s)} \to \pi^{\pm}\mu^+\mu^-$ and $D^{\pm}_{(s)} \to \pi^{\mp}\mu^{\pm}\mu^{\pm}$.

Similar final state topologies; analyses share several common features.
Both analsyes use data taken by LHCb in 2011 at $\sqrt{s} = 7$ TeV.

For LHCb measurements of mixing and CP violation in charm,
see talk by A. Ukleja.

Search for $D^0 \to \mu^+\mu^-$

[LHCb-CONF-2012-005]

$D^0 \to \mu^+\mu^-$

[LHCb-CONF-2012-005]

Very rare in SM; helicity suppression in addition to GIM suppression.
Dominated by long distance contributions from $\gamma\gamma$ intermediate state.
Standard model $\mathcal{B}(D^0 \to \mu^+\mu^-) < 6 \times 10^{-11}$ (90% CL).
Additional constraints from $D^0\bar{D}^0$ mixing measurements
[PRD 79: 114030 (2009)].

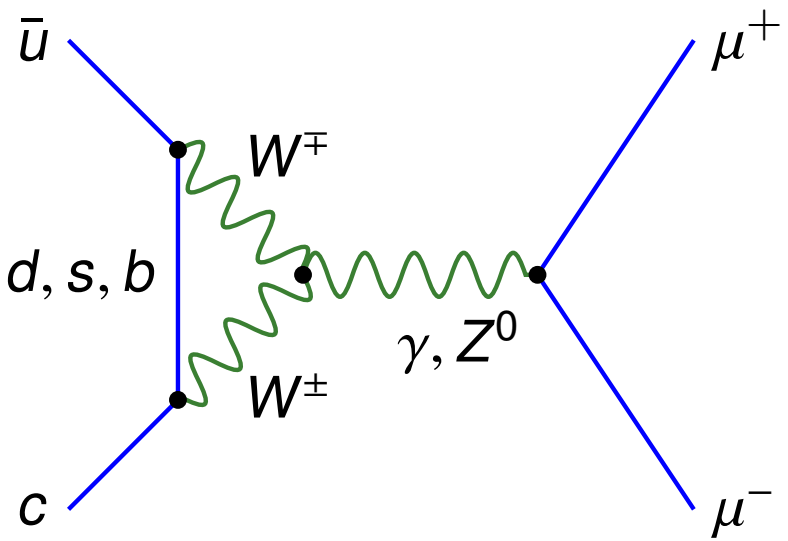

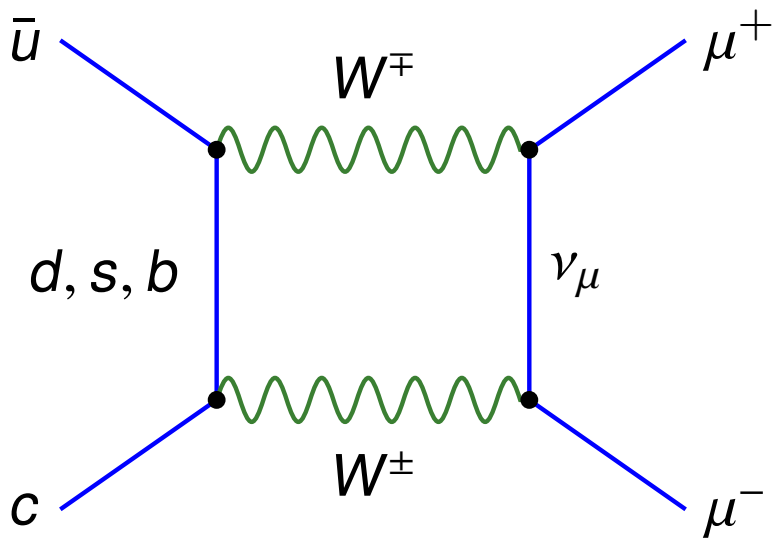

Search for $D^0 \to \mu^+\mu^-$

[LHCb-CONF-2012-005]

LHCb analysis of 0.9 fb^{-1} of data collected in 2011.
Reconstruct $D \to \mu^+\mu^-$ decays produced in prompt $D^{*\pm} \to D\pi_s^\pm$ decays

- Subscript 'S' indicates 'slow'; typically low momentum
- Charge of $\pi_s^\pm$ tags flavour of D
- D^* produced at primary vertex.

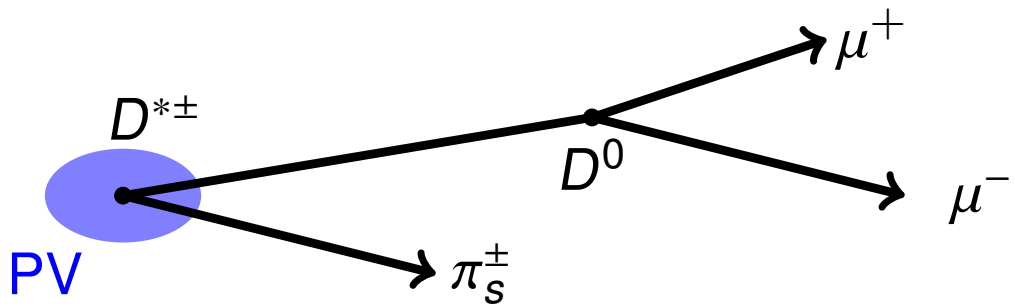

Discriminating variables m_{D^0} and $\Delta m \equiv m_{D^*} - m_{D^0}$.

Search for $D^0 \to \mu^+\mu^-$

[LHCb-CONF-2012-005]

Normalisation channel $D^{*\pm} \to D(\pi^+\pi^-)\pi_s^\pm$

- Very similar kinematics to signal channel.

Yield determined from 2D unbinned ML fit to m_{D^0} (left), Δm (right):

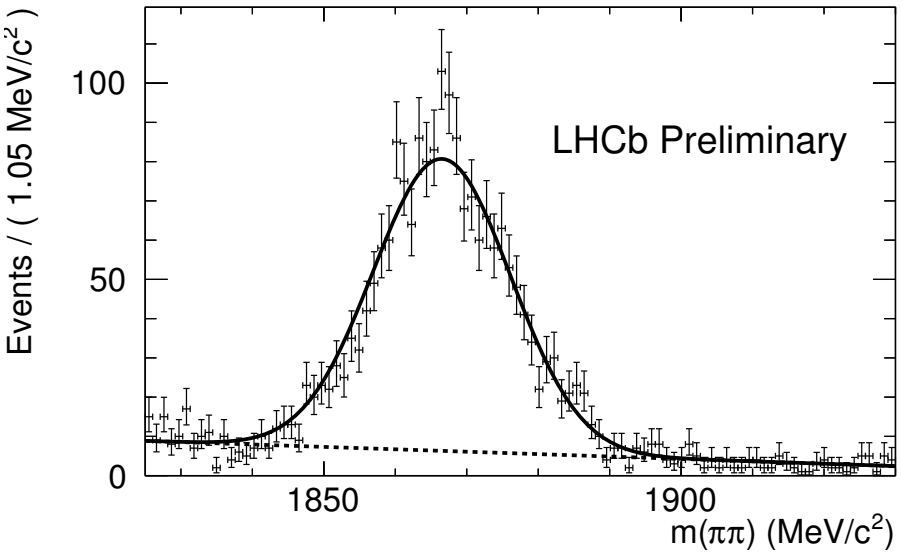

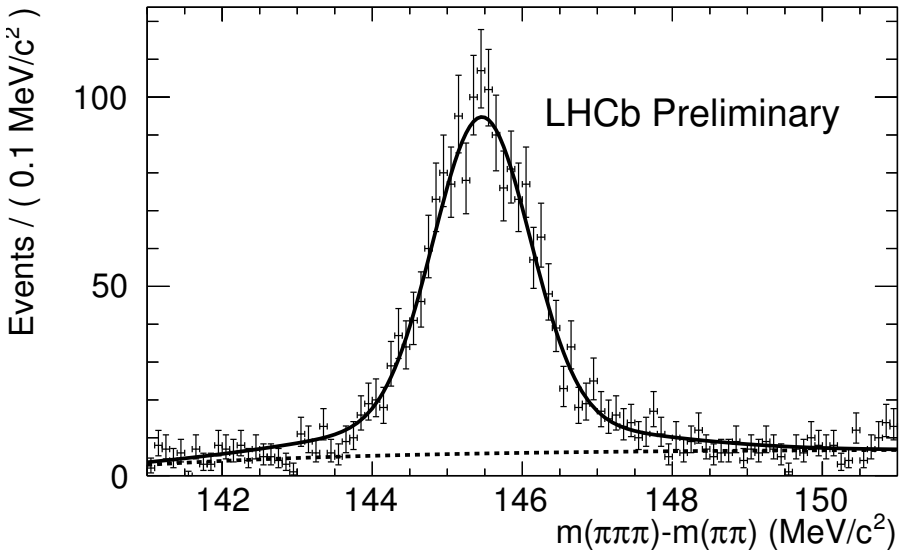

Control channels $J/\psi \to \mu^+\mu^-$ and $D^{*\pm} \to D(K^\pm\pi^\mp)\pi_s^\pm$.

Multivariate selection used to reduce combinatorial background.

Particle ID used to reduce backgrounds in which a π or K is misidentified as a muon.

Determination of $\mathcal{B}(D^0 \to \mu^+\mu^-)$

[LHCb-CONF-2012-005]

$$\mathcal{B}(D^0 \to \mu^+\mu^-) = \frac{N(\mu^+\mu^-)}{N(\pi^+\pi^-)} \times \frac{\varepsilon(\pi^+\pi^-)}{\varepsilon(\mu^+\mu^-)} \times \mathcal{B}(D^0 \to \pi^+\pi^-) = \alpha \times N(\mu^+\mu^-),$$

where α is the 'single event sensitivity'.

Determination of $\mathcal{B}(D^0 \to \mu^+\mu^-)$

[LHCb-CONF-2012-005]

$$\mathcal{B}(D^0 \to \mu^+\mu^-) = \frac{N(\mu^+\mu^-)}{N(\pi^+\pi^-)} \times \frac{\varepsilon(\pi^+\pi^-)}{\varepsilon(\mu^+\mu^-)} \times \mathcal{B}(D^0 \to \pi^+\pi^-) = \alpha \times N(\mu^+\mu^-),$$

where α is the 'single event sensitivity'.

- Trigger and reconstruction efficiencies determined from Monte Carlo simulation and corrected with data-driven methods ($J/\psi \to \mu^+\mu^-$ and $D^{*\pm} \to D(K^\pm\pi^\mp)\pi^\pm_s$ data used).

Determination of $\mathcal{B}(D^0 \to \mu^+\mu^-)$

[LHCb-CONF-2012-005]

$$\mathcal{B}(D^0 \to \mu^+\mu^-) = \frac{N(\mu^+\mu^-)}{N(\pi^+\pi^-)} \times \frac{\varepsilon(\pi^+\pi^-)}{\varepsilon(\mu^+\mu^-)} \times \mathcal{B}(D^0 \to \pi^+\pi^-) = \alpha \times N(\mu^+\mu^-),$$

where α is the 'single event sensitivity'.

- Trigger and reconstruction efficiencies determined from Monte Carlo simulation and corrected with data-driven methods ($J/\psi \to \mu^+\mu^-$ and $D^{*\pm} \to D(K^\pm\pi^\mp)\pi^\pm_s$ data used).
- $N(\pi^+\pi^-)$ determined from 2D unbinned ML fit to $D^{*\pm} \to D(\pi^+\pi^-)\pi^\pm_s$ m_{D^0} and Δm.

Determination of $\mathcal{B}(D^0 \to \mu^+\mu^-)$

[LHCb-CONF-2012-005]

$$\mathcal{B}(D^0 \to \mu^+\mu^-) = \frac{N(\mu^+\mu^-)}{N(\pi^+\pi^-)} \times \frac{\varepsilon(\pi^+\pi^-)}{\varepsilon(\mu^+\mu^-)} \times \mathcal{B}(D^0 \to \pi^+\pi^-) = \alpha \times N(\mu^+\mu^-),$$

where α is the 'single event sensitivity'.

- Trigger and reconstruction efficiencies determined from Monte Carlo simulation and corrected with data-driven methods ($J/\psi \to \mu^+\mu^-$ and $D^{*\pm} \to D(K^\pm\pi^\mp)\pi^\pm_s$ data used).
- $N(\pi^+\pi^-)$ determined from 2D unbinned ML fit to $D^{*\pm} \to D(\pi^+\pi^-)\pi^\pm_s$ m_{D^0} and Δm.
- PDG value of $\mathcal{B}(D^0 \to \pi^+\pi^-)$.

Determination of $\mathcal{B}(D^0 \to \mu^+\mu^-)$

[LHCb-CONF-2012-005]

$$\mathcal{B}(D^0 \to \mu^+\mu^-) = \frac{N(\mu^+\mu^-)}{N(\pi^+\pi^-)} \times \frac{\varepsilon(\pi^+\pi^-)}{\varepsilon(\mu^+\mu^-)} \times \mathcal{B}(D^0 \to \pi^+\pi^-) = \alpha \times N(\mu^+\mu^-),$$

where α is the 'single event sensitivity'.

- Trigger and reconstruction efficiencies determined from Monte Carlo simulation and corrected with data-driven methods ($J/\psi \to \mu^+\mu^-$ and $D^{*\pm} \to D(K^\pm\pi^\mp)\pi^\pm_s$ data used).
- $N(\pi^+\pi^-)$ determined from 2D unbinned ML fit to $D^{*\pm} \to D(\pi^+\pi^-)\pi^\pm_s$ m_{D^0} and Δm.
- PDG value of $\mathcal{B}(D^0 \to \pi^+\pi^-)$.

Determine $\alpha = (1.96 \pm 0.23) \times 10^{-10}$.

Invariant mass and Δm fits

[LHCb-CONF-2012-005]

$D^0 \to \mu^+\mu^-$ mass (left), Δm (right):

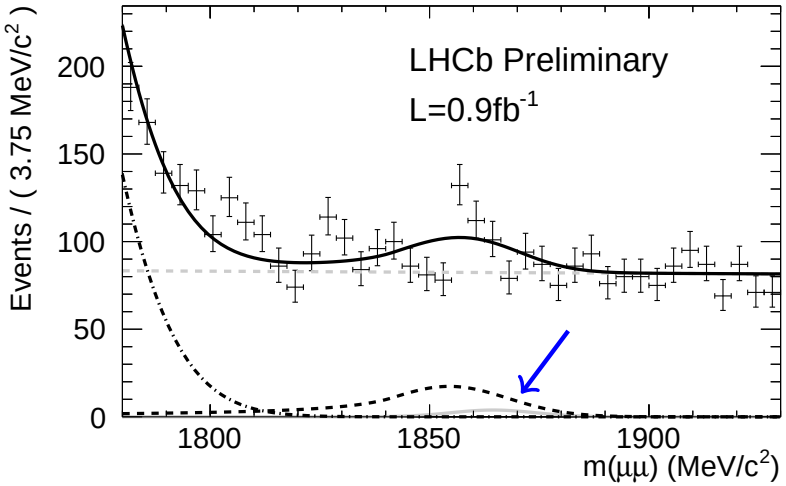

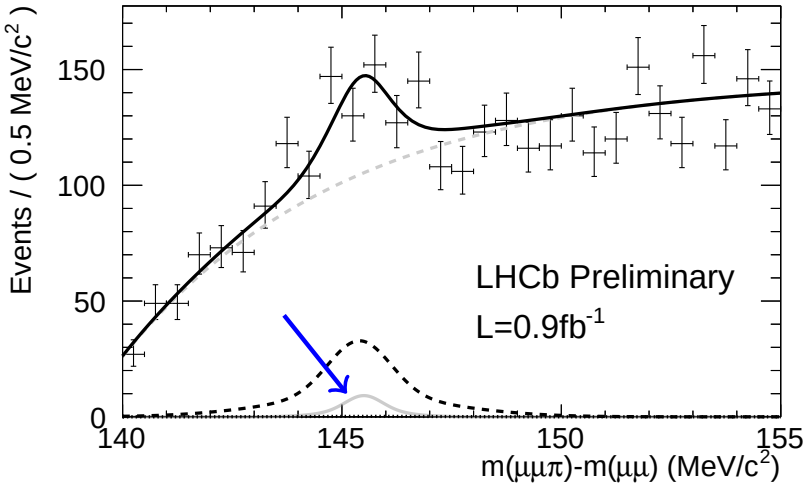

$\mathcal{O}$(8k) candidates. Fit components:

- Signal ——
- $D^0 \to \pi^+\pi^-$ - - - - -
- $D^0 \to K^\pm\pi^\mp$ .....
- Combinatorial background - - - - -

No significant excess over background

Search for $D^0 \to \mu^+\mu^-$

[LHCb-CONF-2012-005]

CL_s method used to determine upper limit on branching fraction:

$$\mathcal{B}(D^0 \to \mu^+\mu^-) < 1.3 \times 10^{-8} \text{ (95\% CL) (preliminary)}$$

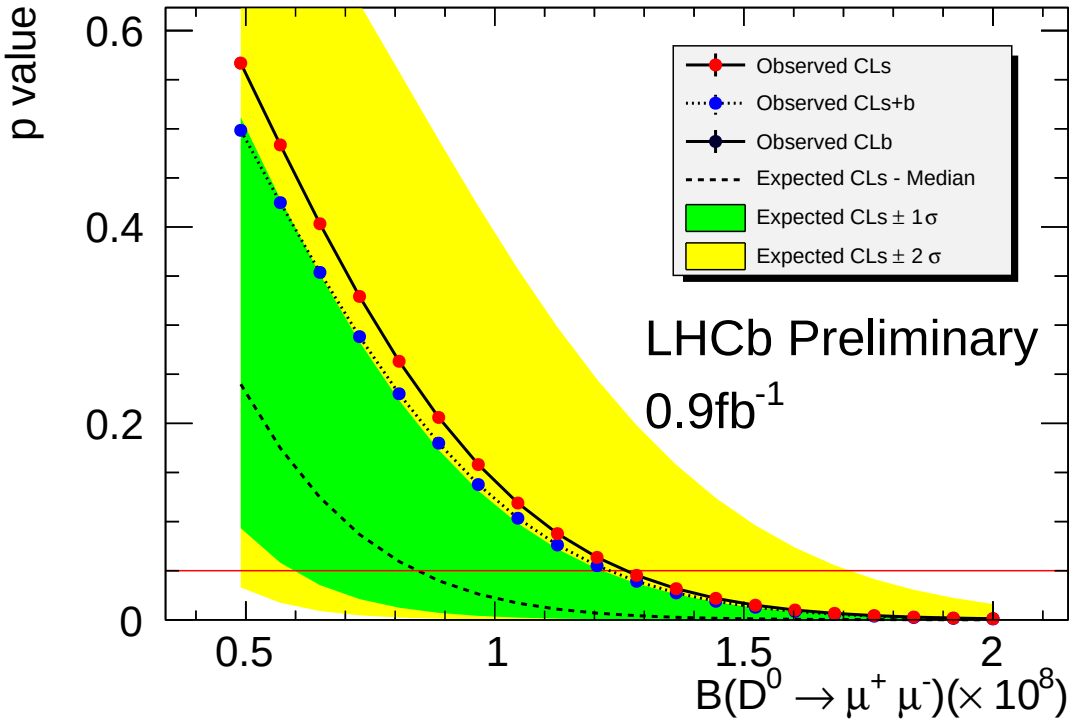

Previous best upper limit 1.4×10^{-7} [PRD 81: 091102(R) (2010)].
SM prediction several orders of magnitude lower.

Search for $D^{\pm}_{(s)} \to \pi^{\pm}\mu^{+}\mu^{-}$ and $D^{\pm}_{(s)} \to \pi^{\mp}\mu^{\pm}\mu^{\pm}$

LHCb-PAPER-2012-051, in preparation

$D^{\pm}_{(s)} \to \pi^{\pm}\mu^{+}\mu^{-}$

LHCb-PAPER-2012-051

Several decays of interest.

1. $D^{\pm} \to \pi^{\pm}\mu^{+}\mu^{-}$

Flavour-changing neutral current.

Expect $\mathcal{B}(c \to u\mu^{+}\mu^{-})$ to be in range 1–3$\times 10^{-9}$

[PRD 83: 114006 (2011)] [PRD 76: 074010 (2007)] [PRD 64: 114009 (2001)].

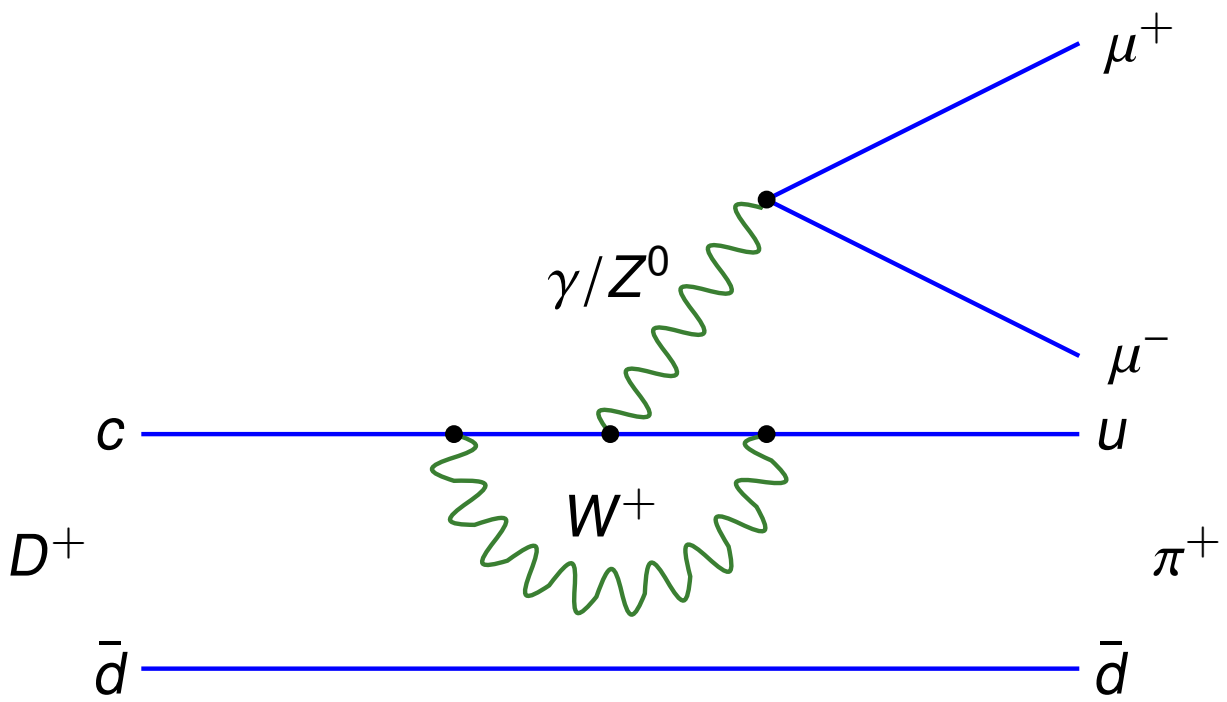

$D^{\pm}_{(s)} \to \pi^{\pm}\mu^{+}\mu^{-}$

LHCb-PAPER-2012-051

Several decays of interest.

2. $D^{\pm}_{s} \to \pi^{\pm}\mu^{+}\mu^{-}$

Proceeds via weak annihilation (WA).

Useful as normalisation;

essential to distinguish WA from FCNC in $D^{\pm} \to \pi^{\pm}\mu^{+}\mu^{-}$.

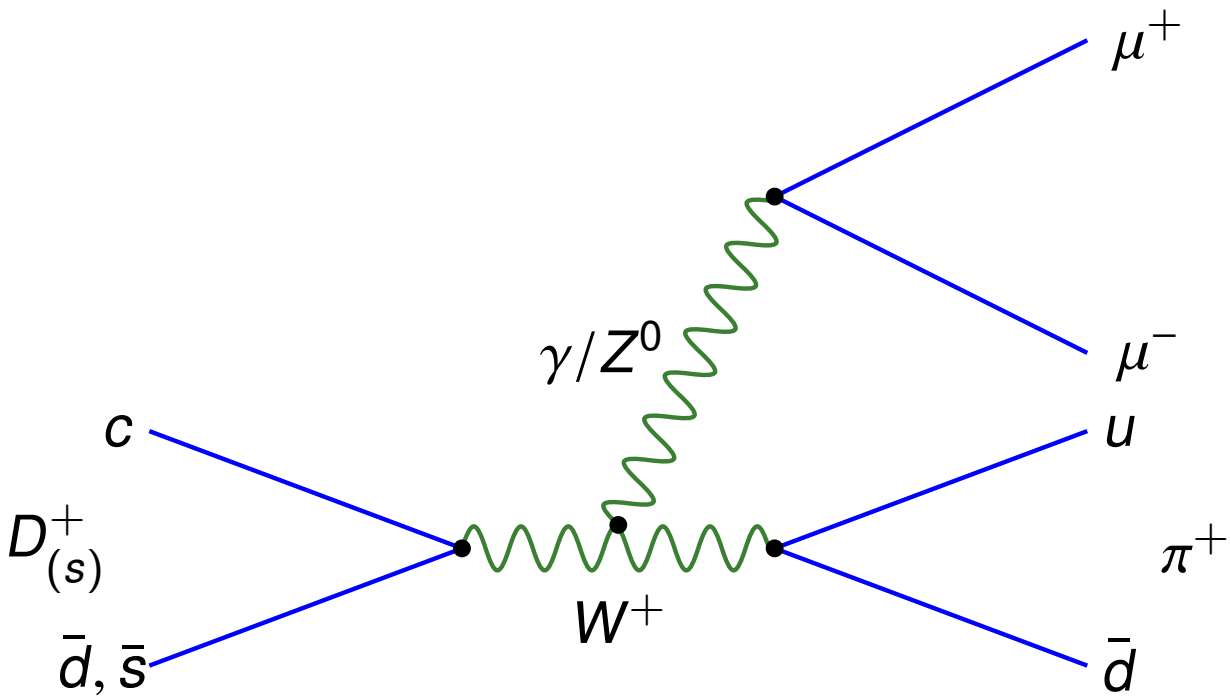

$D^{\pm}_{(s)} \to \pi^{\pm}\mu^{+}\mu^{-}$

LHCb-PAPER-2012-051

Several decays of interest.

3. $D^{\pm}_{(s)} \to \pi^{\mp}\mu^{\pm}\mu^{\pm}$

Lepton number violating process forbidden in SM.

Can only occur by lepton mixing via non-SM particle (e.g. Majorana neutrino).

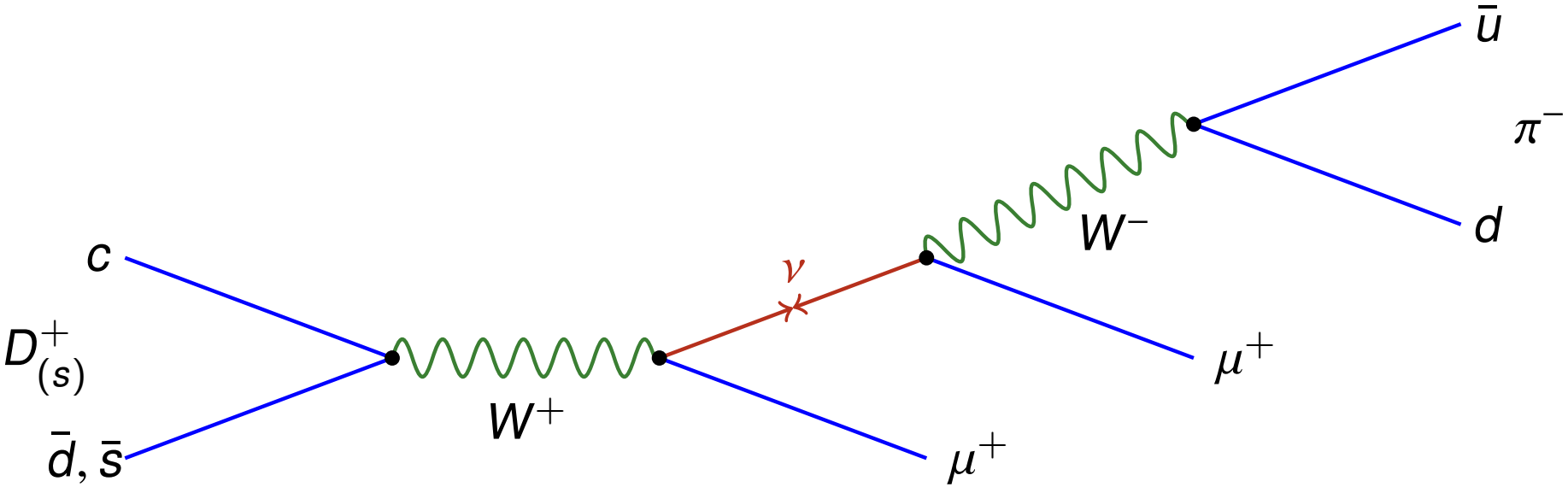

Search for $D^{\pm}_{(s)} \to \pi\mu\mu$

LHCb-PAPER-2012-051

LHCb analysis of 1.0 fb^{-1} of data collected in 2011.
$D^{\pm} \to \pi^{\pm}\phi(\mu^+\mu^-)$ used as normalisation channel.
As with $D^0 \to \mu^+\mu^-$:

- Multivariate algorithm used to distinguish signal from background,
- Particle ID used to ensure the pions and muons are well identified.

Significant background from $D^{\pm}_{(s)} \to \pi^{\mp}\pi^+\pi^-$ decays.

- Independent mass fits performed to determine shape.

Search for $D^{\pm}_{(s)} \to \pi^{\pm}\mu^{+}\mu^{-}$

LHCb-PAPER-2012-051

Large resonant contributions to $\mathcal{B}$ can potentially obscure small signals.
To mitigate, divide $D^{\pm}_{(s)} \to \pi^{\pm}\mu^{+}\mu^{-}$ data divided into kinematic regions:

Low-$m(\mu^{+}\mu^{-})$
250–525 MeV/c^2

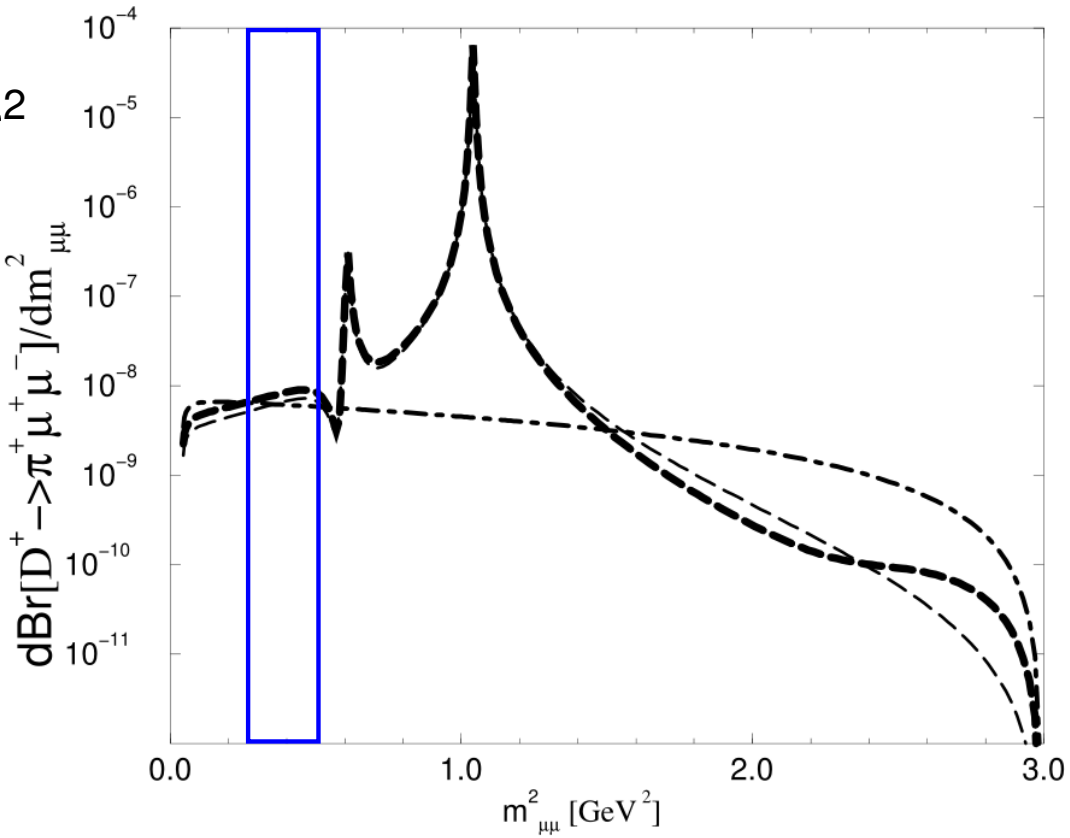

Figure adapted from [PRD 64: 114009 (2001)].

Search for $D^{\pm}_{(s)} \to \pi^{\pm}\mu^{+}\mu^{-}$

LHCb-PAPER-2012-051

Large resonant contributions to $\mathcal{B}$ can potentially obscure small signals.
To mitigate, divide $D^{\pm}_{(s)} \to \pi^{\pm}\mu^{+}\mu^{-}$ data divided into kinematic regions:

η
525–565 MeV/c^2

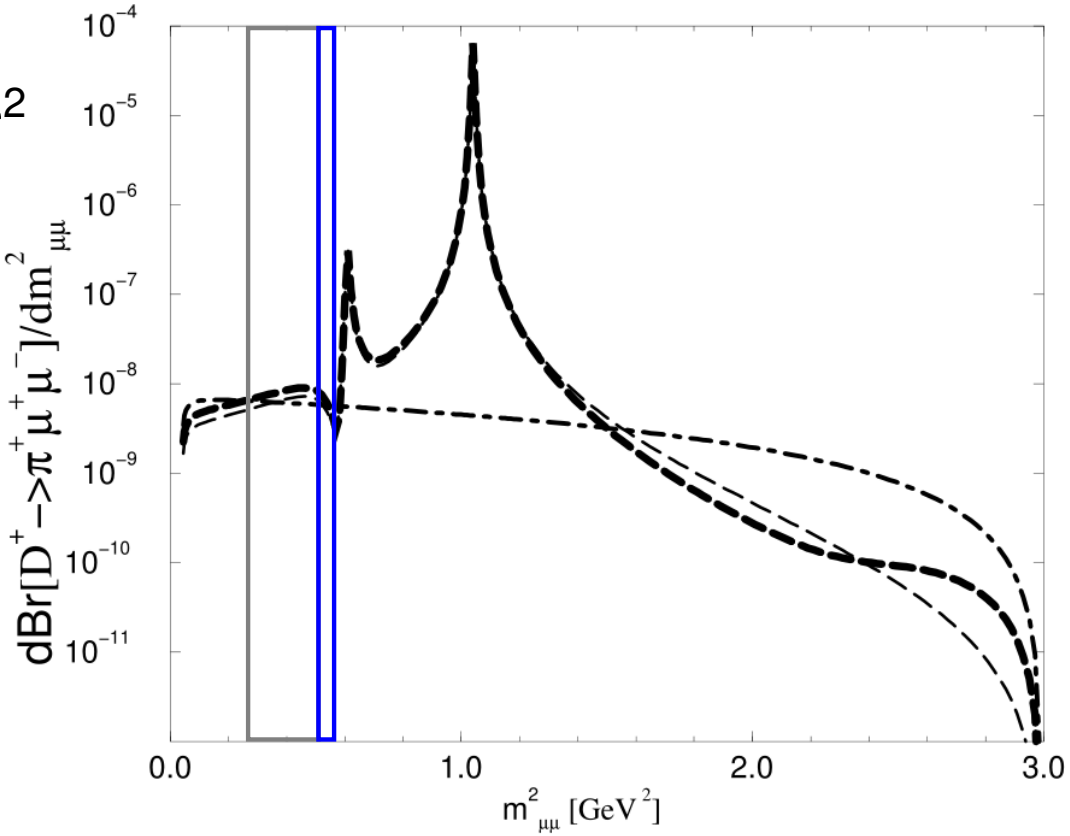

Figure adapted from [PRD 64: 114009 (2001)].

Search for $D^{\pm}_{(s)} \to \pi^{\pm}\mu^{+}\mu^{-}$

LHCb-PAPER-2012-051

Large resonant contributions to $\mathcal{B}$ can potentially obscure small signals.
To mitigate, divide $D^{\pm}_{(s)} \to \pi^{\pm}\mu^{+}\mu^{-}$ data divided into kinematic regions:

ρ/ω
565–850 MeV/c^2

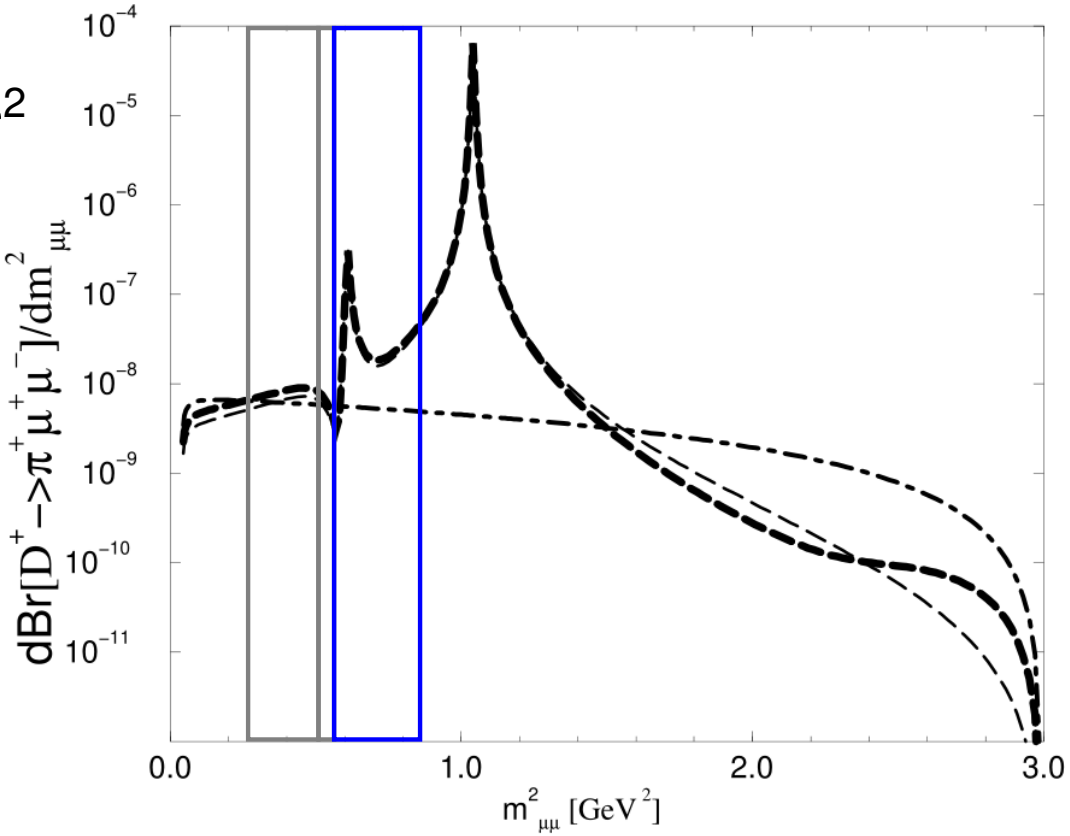

Figure adapted from [PRD 64: 114009 (2001)].

Search for $D^{\pm}_{(s)} \to \pi^{\pm}\mu^{+}\mu^{-}$

LHCb-PAPER-2012-051

Large resonant contributions to $\mathcal{B}$ can potentially obscure small signals.
To mitigate, divide $D^{\pm}_{(s)} \to \pi^{\pm}\mu^{+}\mu^{-}$ data divided into kinematic regions:

ϕ
850–1250 MeV/c^2

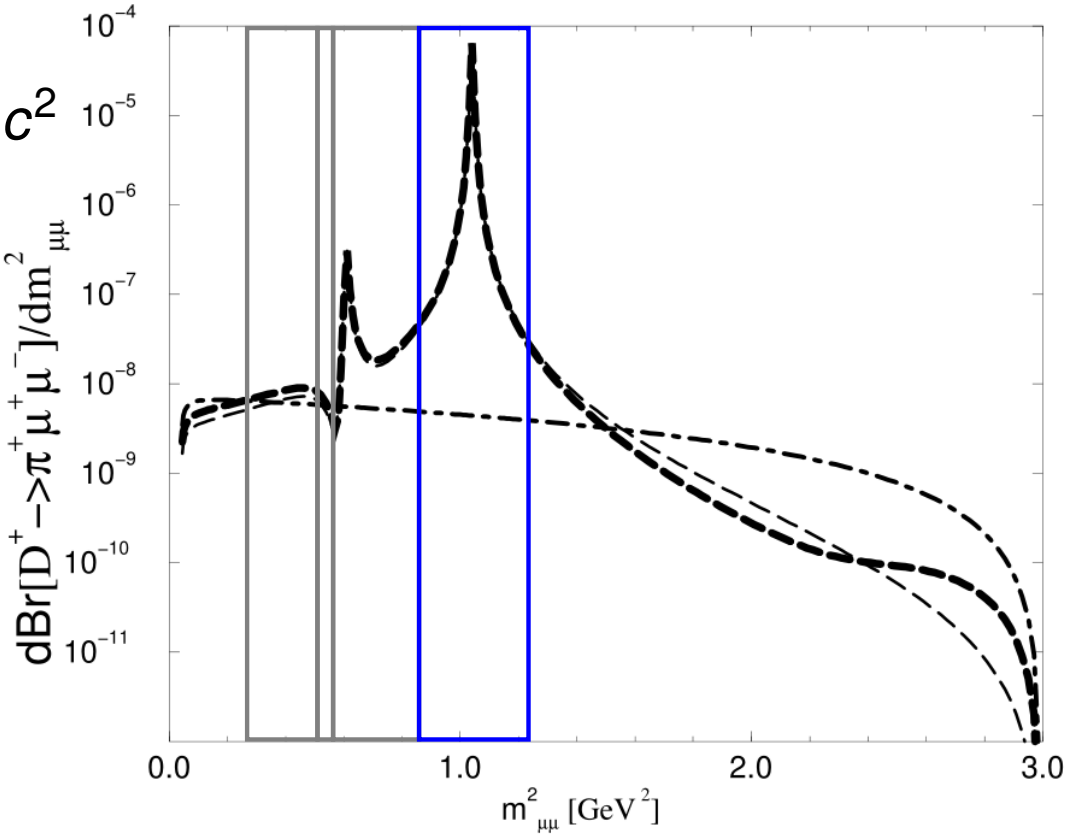

Figure adapted from [PRD 64: 114009 (2001)].

Search for $D^{\pm}_{(s)} \to \pi^{\pm}\mu^{+}\mu^{-}$

LHCb-PAPER-2012-051

Large resonant contributions to $\mathcal{B}$ can potentially obscure small signals.
To mitigate, divide $D^{\pm}_{(s)} \to \pi^{\pm}\mu^{+}\mu^{-}$ data divided into kinematic regions:

High-$m(\mu^{+}\mu^{-})$
1250–2000 MeV/c^2

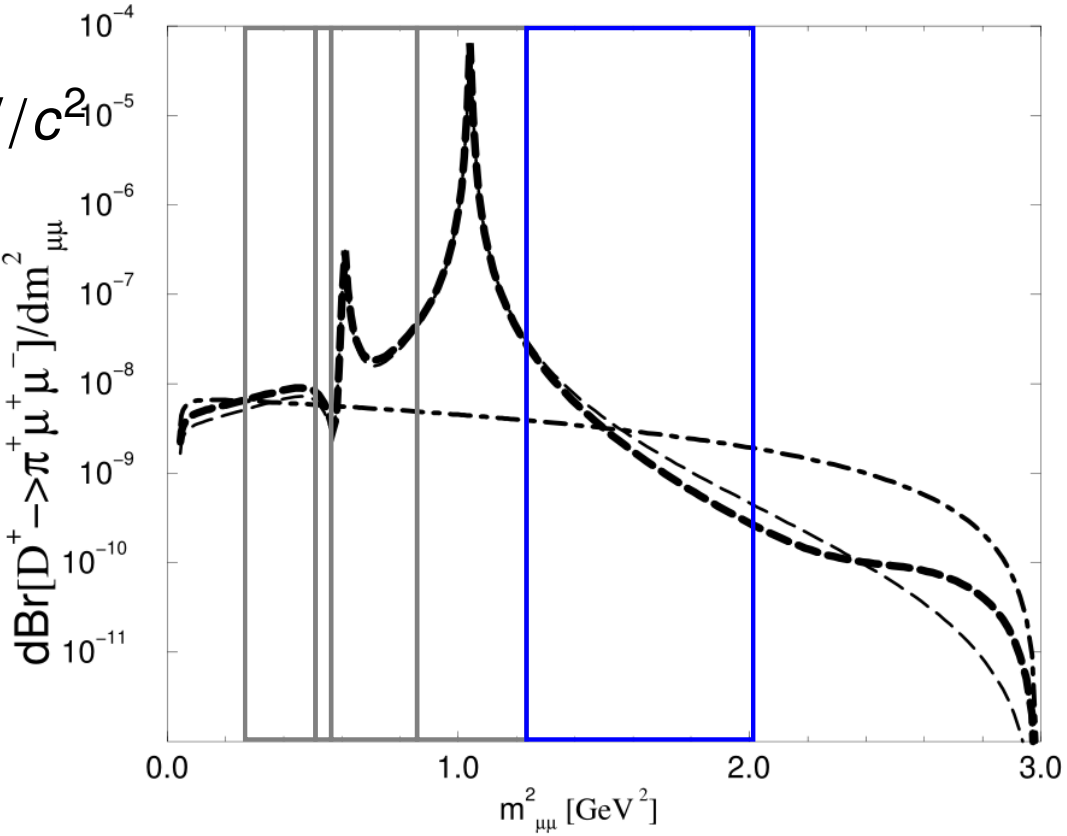

Figure adapted from [PRD 64: 114009 (2001)].

$D^{\pm}_{(s)} \to \pi^{\pm}\mu^{+}\mu^{-}$ invariant mass fits

LHCb-PAPER-2012-051

Binned ML fit performed in each kinematic bin, sharing some parameters between bins

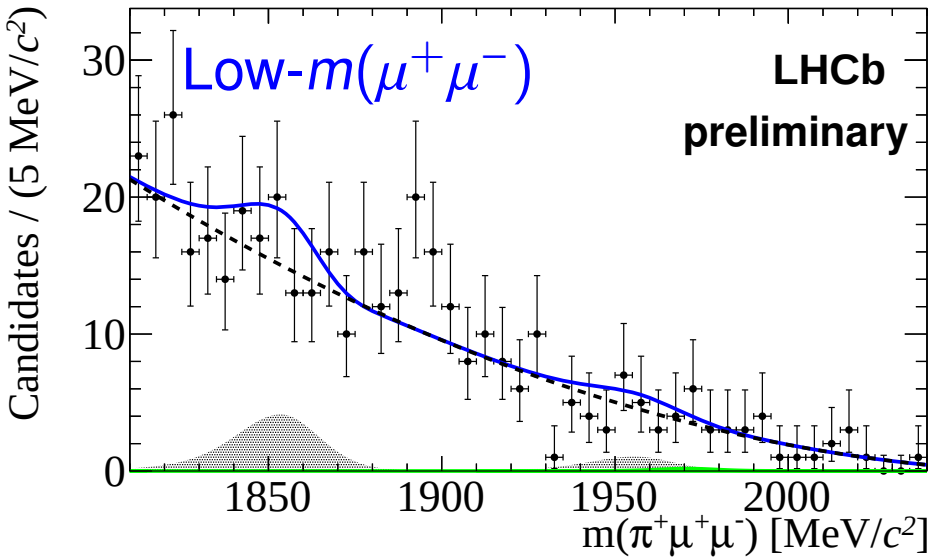

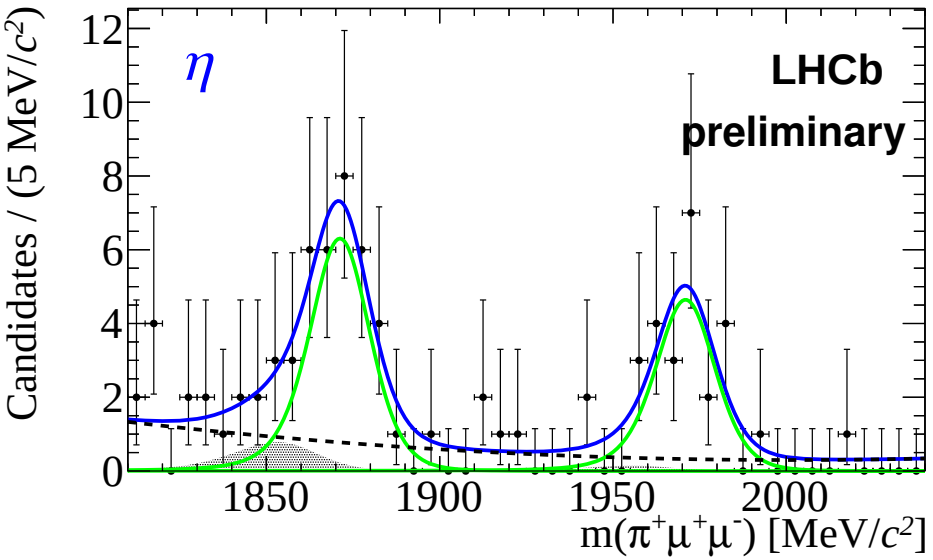

- Total PDF
- Signal
- Peaking background
- Non-peaking background

$$\mathcal{B}(D^{\pm}_{(s)} \to \eta(\mu^+\mu^-)\pi^{\pm}) \sim 10^{-8}$$

$D^{\pm}_{(s)} \to \pi^{\pm}\mu^{+}\mu^{-}$ invariant mass fits

LHCb-PAPER-2012-051

Binned ML fit performed in each kinematic bin, sharing some parameters between bins

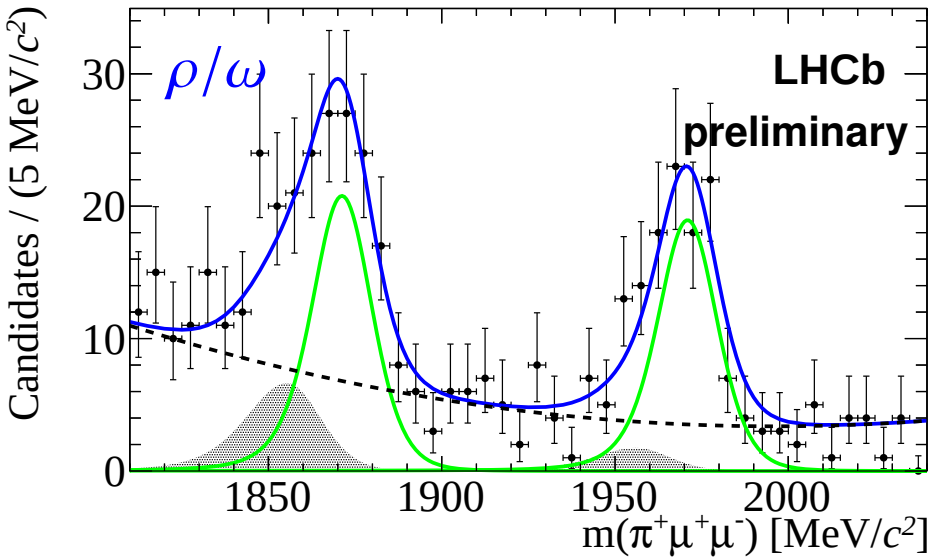

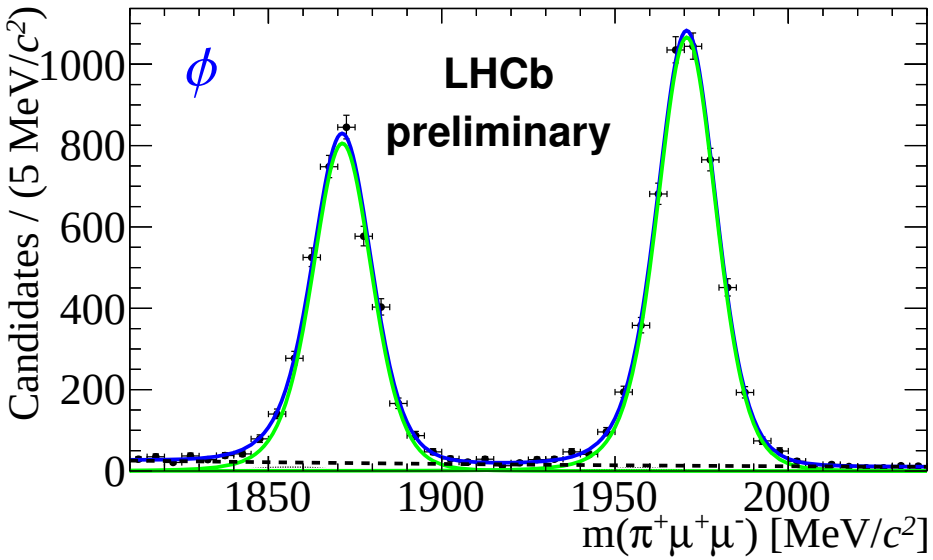

- Total PDF
- Signal
- Peaking background
- Non-peaking background

Abundant normalisation channel

$D^{\pm}_{(s)} \to \pi^{\pm}\mu^{+}\mu^{-}$ invariant mass fits

LHCb-PAPER-2012-051

Binned ML fit performed in each kinematic bin, sharing some parameters between bins

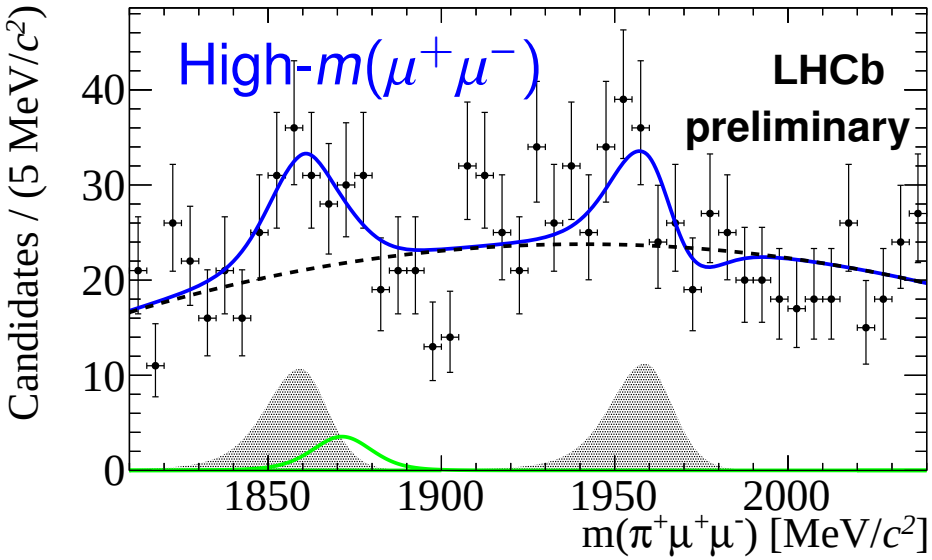

- Total PDF
- Signal
- Peaking background
- Non-peaking background

Conclusions:

Clear signals in resonant regions.

No significant non-resonant signal in high/low $m(\mu^+\mu^-)$ bins

Search for $D^{\pm}_{(s)} \to \pi^{\mp}\mu^{\pm}\mu^{\pm}$

LHCb-PAPER-2012-051

$D^{\pm}_{(s)} \to \pi^{\mp}\mu^{\pm}\mu^{\pm}$ data also binned to improve signal significance; assume Majorana neutrino signal will only appear in one bin.
Divide data into four bins of $m(\mu^{\pm}\pi^{\mp})$:

1. 250–1140 MeV/c^2,
2. 1140–1340 MeV/c^2,
3. 1340–1550 MeV/c^2,
4. 1540–2000 MeV/c^2.

$D^{\pm}_{(s)} \to \pi^{\mp}\mu^{\pm}\mu^{\pm}$ invariant mass fits

LHCb-PAPER-2012-051

Binned ML fit performed in each kinematic bin, sharing some parameters between bins

$m(\mu^{\pm}\pi^{\mp})$ bins 1 and 2:

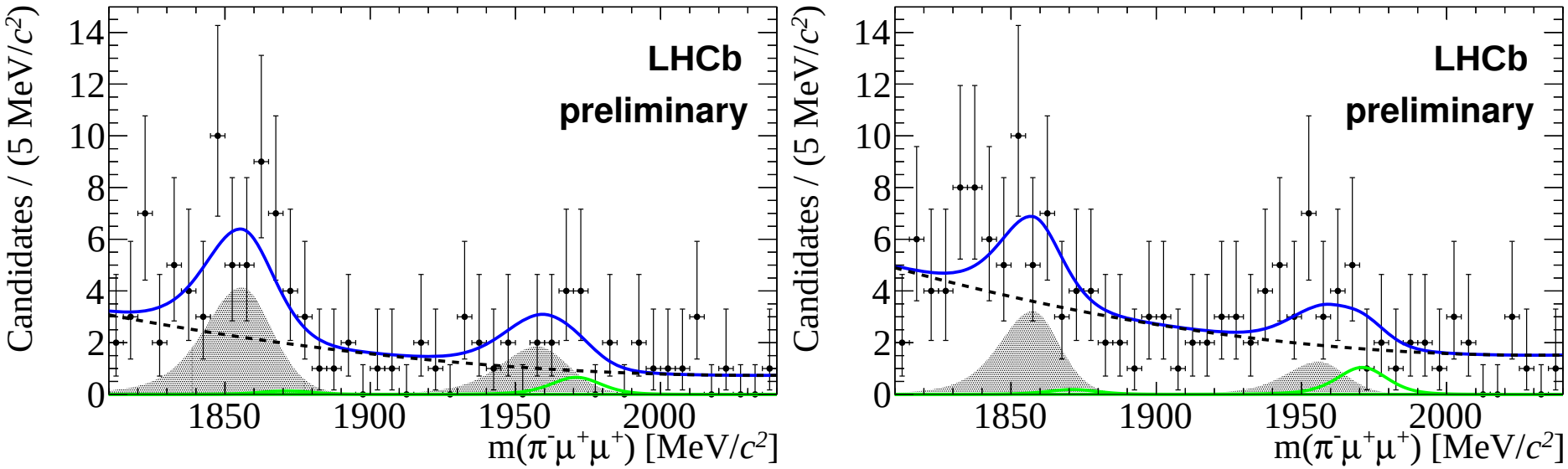

- Total PDF
- Signal
- Peaking background
- Non-peaking background

$D^{\pm}_{(s)} \to \pi^{\mp}\mu^{\pm}\mu^{\pm}$ invariant mass fits

LHCb-PAPER-2012-051

Binned ML fit performed in each kinematic bin, sharing some parameters between bins

$m(\mu^{\pm}\pi^{\mp})$ bins 3 and 4:

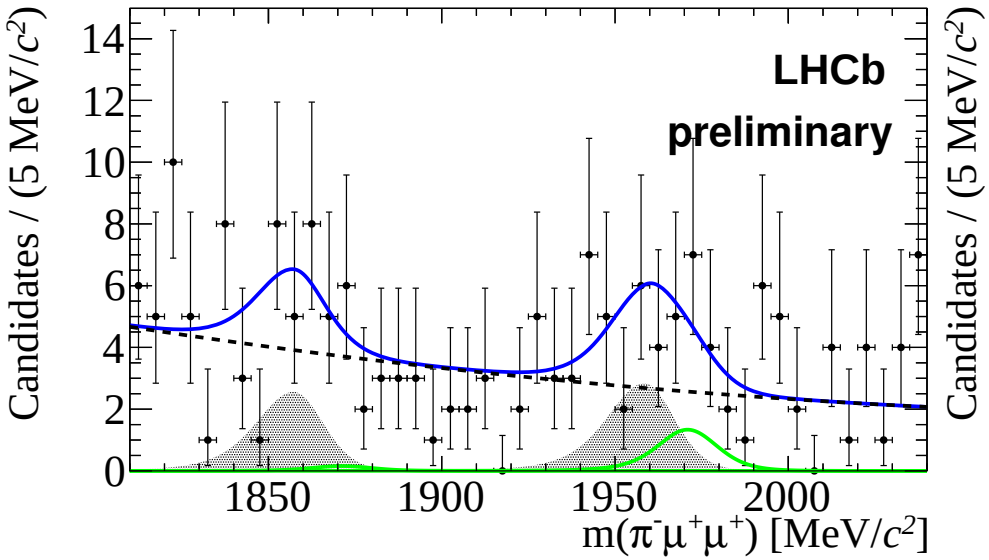

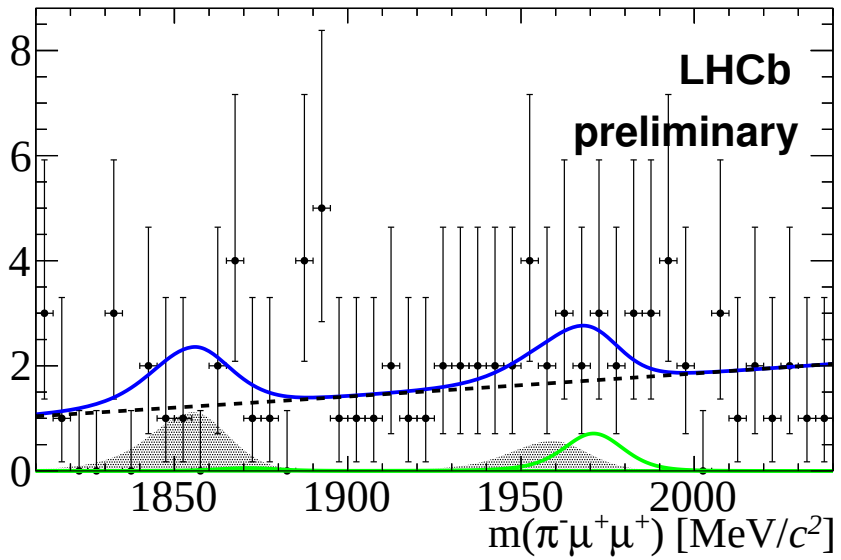

- Total PDF
- Signal
- Peaking background
- Non-peaking background

Conclusion:
No excess over background observed.

Determination of $\mathcal{B}(D^{\pm}_{(s)} \to \pi\mu\mu)$

LHCb-PAPER-2012-051

No significant excess over background for either decay mode.

Branching fraction

$$\mathcal{B}(D^{\pm}_{(s)} \to \pi\mu\mu) = \frac{N(D^{\pm}_{(s)} \to \pi\mu\mu)}{N(D^{\pm}_{(s)} \to \phi(\mu^+\mu^-)\pi)} \times \frac{\varepsilon(D^{\pm}_{(s)} \to \phi(\mu^+\mu^-)\pi)}{\varepsilon(D^{\pm}_{(s)} \to \pi\mu\mu)} \times \mathcal{B}(D^{\pm}_{(s)} \to \phi(\mu^+\mu^-)\pi)$$

As with $D^0 \to \mu^+\mu^-$:

- Efficiencies from simulation corrected by data-driven methods,
- $N(D^{\pm}_{(s)} \to \phi(\mu^+\mu^-)\pi)$ from fits to normalisation channel in ϕ bin,
- $\mathcal{B}(D^{\pm}_{(s)} \to \phi(\mu^+\mu^-)\pi)$ from PDG.

Search for $D^{\pm} \to \pi^{\pm}\mu^{+}\mu^{-}$

LHCb-PAPER-2012-051

CL_s method used to determine upper limit on branching fraction:

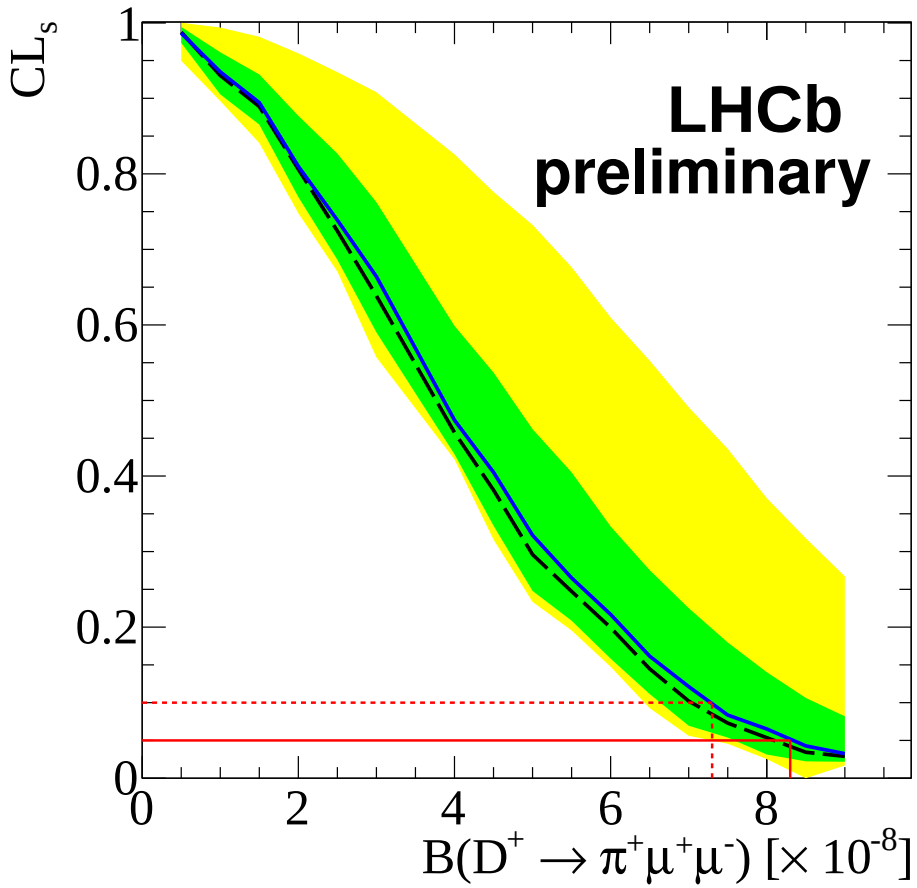

Observed — Expected — Bkg-only, 1σ — Bkg-only, 2σ — Upper limit, 90% CL ····· Upper limit, 95% CL —

Search for $D^{\pm}_{(s)} \to \pi\mu\mu$

LHCb-PAPER-2012-051

Observed limits compatible with background-only hypothesis.
Preliminary results at 95% CL, excluding resonant regions:

$$\mathcal{B}(D^{\pm} \to \pi^{\pm}\mu^{+}\mu^{-}) < 8.3 \times 10^{-8},$$
$$\mathcal{B}(D_s^{\pm} \to \pi^{\pm}\mu^{+}\mu^{-}) < 4.8 \times 10^{-7},$$
$$\mathcal{B}(D^{\pm} \to \pi^{\mp}\mu^{\pm}\mu^{\pm}) < 2.5 \times 10^{-8},$$
$$\mathcal{B}(D_s^{\pm} \to \pi^{\mp}\mu^{\pm}\mu^{\pm}) < 1.4 \times 10^{-7}.$$

New!

Previous best limit for $\mu^{+}\mu^{-}$ channel:

- DØ: $\mathcal{B}(D^{\pm} \to \pi^{\pm}\mu^{+}\mu^{-}) < 3.9 \times 10^{-6}$ (90% CL) [PRL 100: 101801 (2008)],
- BaBar: $\mathcal{B}(D^{\pm} \to \pi^{\pm}\mu^{+}\mu^{-}) < 6.5 \times 10^{-6}$ (90% CL) [hep-ex/1107.4465].

Previous best limit for $\mathcal{B}(D^{\pm} \to \pi^{\mp}\mu^{\pm}\mu^{\pm}) < 2 \times 10^{-6}$ (90% CL), BaBar [hep-ex/1107.4465].

Conclusions

- Rare charm decays are a promising way to reveal the presence of BSM physics.
- LHCb analyses of 2011 data:
  1. $D^0 \to \mu^+\mu^-$,
  2. $D^{\pm}_{(s)} \to \pi^{\pm}\mu^+\mu^-$ and $D^{\pm}_{(s)} \to \pi^{\mp}\mu^{\pm}\mu^{\pm}$.
- Upper limits on $\mathcal{B}$ set for each final state
  - $\mathcal{O}$(10–100) improvement over previous best measurements,
  - Not yet enough data to reach SM sensitivity.
- Updates incorporating 2012 data planned.
- Similar decays of interest, e.g.:
  - $K^+K^-\mu^+\mu^-$,
  - $K^*\mu^+\mu^-$,
  - $D^0 \to e^{\pm}\mu^{\mp}$ (LNV).

Backup

The LHCb trigger

LHCb trigger consists of two principal stages:

- Hardware trigger (L0): takes information from calorimeter and muon stations. High $E_T/\mathbf{p}_T$ signatures. Reduces LHC rate to ~ 1 MHz.
- Software trigger (HLT): algorithms designed to select decays of interest based on typical features. Two sub-stages (HLT1, HLT2). Inclusive and exclusive algorithms. Reduces rate to ~ 3 kHz, of which $\sim 1/3$ is charm decays.

Muonic triggers:

- L0: one muon with $\mathbf{p}_T > 1.5$ GeV$/c$, or two muons with $\sqrt{\mathbf{p}_T^1 \times \mathbf{p}_T^2} > 1.3$ GeV$/c$
- HLT single muon trigger: one track identified as a muon, $\mathbf{p}_T > 1$ GeV$/c$, PV IP > 0.1mm
- HLT dimuon trigger: two oppositely charged tracks both identified as muons, good track quality, vertex with mass > 1 GeV$/c^2$, $\mathbf{p}_T > 0.5$ GeV$/c$, $\mathbf{p} > 6$ GeV$/c$

$D^0 \to \mu^+\mu^-$ selection criteria

D^0 daughters: good quality, high $\mathbf{p}_T$ tracks displaced from PV, fulfil muon ID requirements.
D^0: good vertex fit, high $\mathbf{p}_T$, displaced from PV and pointing towards PV, loose mass requirements.
π_s: small IP with respect to PV, $\mathbf{p}_T$ cut.
D^*: cut on Δm, constraining slow pion towards PV
Boosted Decision Tree with $\sim$ 10 variables, trained on simulated signal and data sideband backgrounds. Data not used in further fits.

$D^0 \to \mu^+\mu^-$ fit components

Δm: double Gaussian with common mean for signal, empirical shape for combinatorial and $\pi^+\pi^-$ backgrounds, Gaussian for $K^\pm\pi^\mp$ background.
m_{D^0}: Crystal Ball for signal, exponential for combinatorial and $K^\pm\pi^\mp$ backgrounds, Crystal Ball for $\pi^+\pi^-$ background.

$D^0 \to \mu^+\mu^-$ correction of simulated data

Trigger efficiencies:

- Use $J/\psi \to \mu^+\mu^-$ events in data and simulation to check agreement for signal channel; consitent within uncertainties.
- Use $D^0 \to K^\pm\pi^\mp$ events in data and simulation to check agreement for normalisation channel; correction applied.
- Muon ID efficiency determined with MC and validated with $J/\psi \to \mu^+\mu^-$ data; small correction applied.

Reconstruction efficiencies:

- MC-data differences determined with tagged $K^\pm\pi^\mp$ data.
- Additional systematic uncertainty due to differences in material interactions (μ/π).

$D^0 \to \mu^+\mu^-$ systematic uncertainties

Systematic uncertainties from:

- Normalisation (α),
- Background description,
- Triggers (hadron and muon).

Propagated to final result by applying constraints in fit.

$D^{\pm}_{(s)} \to \pi\mu\mu$ selection criteria

$D^{\pm}_{(s)}$ daughter $\pi^{\pm}$: high **p** and $\mathbf{p}_{\mathrm{T}}$, good track quality, displaced from PV, not identified as muon

$D^{\pm}_{(s)}$ daughter $\mu^{\pm}$: positive ID as muon, isolated in muon detectors

$D^{\pm}_{(s)}$: good vertex quality, pointing towards PV, loose mass requirements, isolation

BDT with $\sim$ 10 variables, trained on simulated signal and 2010 data sidebands.

$D^{\pm}_{(s)} \to \pi\mu\mu$ fit components

Signal: Gaussian with modified tails.
$\pi\pi\pi$ peaking background: Gaussian with modified tails.
Non-peaking background: second-order polynomial.

$D^{\pm}_{(s)} \to \pi\mu\mu$ correction of simulated data

$B \to J/\psi X$ decays used to compare simulation and data; compare tracking and muon ID efficiency differences.
Pion identification studied using D^*-tagged $K^{\pm}\pi^{\mp}$ data.

$D^{\pm}_{(s)} \to \pi\mu\mu$ systematic uncertainties

Systematic uncertainties from:

- Control mode $\mathcal{B}$,
- Signal and background shapes,
- MC-data differences,
- Tracking,
- PID.

Incorporated following the prescription in JPG 28, no 10: 2693 (2002) and NIM A 434: 435 (1999).